Since January 2020 Elsevier has created a COVID-19 resource centre with free information in English and Mandarin on the novel coronavirus COVID-19. The COVID-19 resource centre is hosted on Elsevier Connect, the company's public news and information website.

Biomaterials 267 (2021) 120389

Contents lists available at ScienceDirect

Biomaterials

journal homepage: www.elsevier.com/locate/biomaterials

Long-acting nanoparticulate DNase-1 for effective suppression of SARS-CoV-2-mediated neutrophil activities and cytokine storm

Yun Young Lee [a,1], Hee Ho Park [b,1], Wooram Park [c,1], Hyelim Kim [d,1], Jong Geol Jang [e], Kyung Soo Hong [e], Jae-Young Lee [d], Hee Seung Seo [f], Dong Hee Na [g], Tae-Hyung Kim [h], Young Bin Choy [a], June Hong Ahn [e,***], Wonhwa Lee [i,**], Chun Gwon Park [f,j,k,l,*]

[a] Department of Biomedical Engineering, Seoul National University College of Medicine, Seoul, 03080, Republic of Korea
[b] Department of Biotechnology and Bioengineering, Kangwon National University, Chuncheon, Gangwon-do, 24341, Republic of Korea
[c] Department of Biomedical-Chemical Engineering, The Catholic University of Korea, Bucheon, 14662, Republic of Korea
[d] College of Pharmacy, Chungnam National University, Daejeon, 34134, Republic of Korea
[e] Division of Pulmonary and Allergy, Department of Internal Medicine, College of Medicine, Yeungnam University and Regional Center for Respiratory Diseases, Yeungnam University Medical Center, Daegu, 42415, Republic of Korea
[f] Department of Biomedical Engineering, SKKU Institute for Convergence, Sungkyunkwan University (SKKU), Suwon, 16419, Republic of Korea
[g] College of Pharmacy, Chung-Ang University, Seoul, 06974, Republic of Korea
[h] School of Integrative Engineering, Chung-Ang University, Seoul, 06974, Republic of Korea
[i] Aging Research Center, Korea Research Institute of Bioscience and Biotechnology, Daejeon, 34141, Republic of Korea
[j] Biomedical Institute for Convergence at SKKU (BICS), Sungkyunkwan University, Suwon, 16419, Republic of Korea
[k] Department of Intelligent Precision Healthcare Convergence, SKKU Institute for Convergence, Sungkyunkwan University (SKKU), Suwon 16419, Republic of Korea
[l] Center for Neuroscience Imaging Research, Institute for Basic Science (IBS), Suwon 16419, Republic of Korea

ARTICLE INFO

Keywords:
COVID-19
Sepsis
DNase
Nanoparticles
NETosis

ABSTRACT

Severe acute respiratory syndrome coronavirus 2 (SARS-CoV-2) is a new strain of coronavirus not previously identified in humans. Globally, the number of confirmed cases and mortality rates of coronavirus disease 2019 (COVID-19) have risen dramatically. Currently, there are no FDA-approved antiviral drugs and there is an urgency to develop treatment strategies that can effectively suppress SARS-CoV-2-mediated cytokine storms, acute respiratory distress syndrome (ARDS), and sepsis. As symptoms progress in patients with SARS-CoV-2 sepsis, elevated amounts of cell-free DNA (cfDNA) are produced, which in turn induce multiple organ failure in these patients. Furthermore, plasma levels of DNase-1 are markedly reduced in SARS-CoV-2 sepsis patients. In this study, we generated recombinant DNase-1-coated polydopamine-poly(ethylene glycol) nanoparticulates (named long-acting DNase-1), and hypothesized that exogenous administration of long-acting DNase-1 may suppress SARS-CoV-2-mediated neutrophil activities and the cytokine storm. Our findings suggest that exogenously administered long-acting nanoparticulate DNase-1 can effectively reduce cfDNA levels and neutrophil activities and may be used as a potential therapeutic intervention for life-threatening SARS-CoV-2-mediated illnesses.

1. Introduction

There is a massive concern regarding the outbreak of coronavirus disease 2019 (COVID-19) caused by the highly infectious and lethal severe acute respiratory syndrome coronavirus 2 (SARS-CoV-2) [1]. The COVID-19 pandemic is a severe threat to public health across the globe. Current statistics report approximately 250,000 deaths and more than 3,500,000 confirmed cases in 180 countries worldwide [2], but the

* Corresponding author. Department of Biomedical Engineering, SKKU Institute for Convergence, Sungkyunkwan University (SKKU), Suwon, 16419, Republic of Korea.
** Corresponding author. Aging Research Center, Korea Research Institute of Bioscience and Biotechnology, Daejeon 34141 Republic of Korea
*** Corresponding author. Division of Pulmonary and Allergy, Department of Internal Medicine, College of Medicine, Yeungnam University and Regional Center for Respiratory Diseases, Yeungnam University Medical Center, Daegu, 42415, Republic of Korea
E-mail addresses: fireajh@yu.ac.kr (J.H. Ahn), wonhwalee@kribb.re.kr (W. Lee), chunpark@skku.edu (C.G. Park).
[1] These authors contributed equally as first authors: Yun Young Lee, Hee Ho Park, Wooram Park, Hyelim Kim.

https://doi.org/10.1016/j.biomaterials.2020.120389
Received 19 June 2020; Received in revised form 7 September 2020; Accepted 16 September 2020
Available online 23 October 2020

situation is highly fluid and the numbers continue to rise. Experts are forecasting hundreds of thousands of mortalities worldwide.

SARS-CoV-2 infections are associated with both impaired adaptive immune responses and uncontrolled inflammatory innate immune responses, which lead to local and systemic tissue damage [1]. The radical immune reactions cause septic shock which lead to increase in the mortality rates of patients [1]. Thus, there is an urgent need to develop new treatment strategies that can suppress the progression of SARS-CoV-2-induced sepsis. Many research groups and global pharmaceutical companies have been conducting intense preclinical and phase I trials of potential SARS-CoV-2 treatments [3–5]. However, most of these drugs have not been developed for the actual treatment of SARS-CoV-2, but rather were developed for the treatment of other viruses, such as Ebola virus, human immunodeficiency virus (HIV), severe acute respiratory syndrome (SARS) virus, Middle East respiratory syndrome (MERS) virus, Influenza A virus, and ZIKA virus [6]. Various clinical studies have shown that suppression of cytokine release syndrome (CRS) and respiratory damage are substantial hurdles needed to be overcome in severely affected patients [2,7]. Recently, Genentech has announced FDA approval of phase III clinical trial for Tocilizumab (Actemra) to treat hospitalized patients with severe SARS-CoV-2 pneumonia (NCT04320615) [8]. However, even after the successful resolution of the virus infection, patients may not exhibit full recovery from the damage and may progress to more severe disease, such as acute respiratory distress syndrome (ARDS) and sepsis, or in worse cases, death. Currently, the World Health Organization (WHO) does not recommend corticosteroids for the treatment of patients with COVID-19, as they may exacerbate SARS-CoV-2-associated acute respiratory infections [9]. Since acute complications and fatalities are associated with the virus, new strategies are urgently needed to address the rapid respiratory-related inflammatory responses.

Neutrophil extracellular traps (NETs) are reticular structures consisting of a DNA backbone and a number of functional proteins that are formed through a process known as NETosis [10,11]. NETs exert anti-infective activity by capturing pathogenic microorganisms (including viruses), preventing their spread, and by inactivating pathogenic factors. However, it has been reported that immune responses caused by NETosis may also induce tissue damage [12]. SARS-CoV-2 infections may impair adaptive immune responses as well as induce uncontrolled inflammatory innate immune responses, which cause local and systemic tissue damage. These phenomena are typically associated with elevated levels of NETosis markers, such as cell-free DNA (cfDNA), myeloperoxidase (MPO), and neutrophil elastase (NE). These factors correlate with increased disease severity and poor clinical outcome. It is particularly challenging to treat patients that exhibit high levels of NETosis. Consistent with this, an approach that inhibits NETosis has significantly increased the survival in pulmonary sepsis [13,14].

In the current study, we sought to determine if NETosis markers were actually increased in patients infected with SARS-CoV-2 and whether suppressing NETs could be used as a possible treatment approach for acute respiratory infections associated with COVID-19. We analyzed NETosis makers in the blood of patients with COVID-19 to determine the association of NETosis with the acute immune response triggered by SARS-CoV-2. We showed that an intravenous administration of DNase-1-coated polydopamine-poly (ethylene glycol) nanoparticulates, named long-acting DNase-1 (Scheme 1), effectively inhibited NETosis factors in blood samples of patients with COVID-19 and also improve survival in a sepsis model. Currently, there are no FDA-approved therapeutic agents available for treating patients infected with SARS-CoV-2. Monitoring and modulation of NETosis are novel strategies in the diagnosis and treatment of patients with COVID-19 and may ultimately contribute to the development of therapeutic agents.

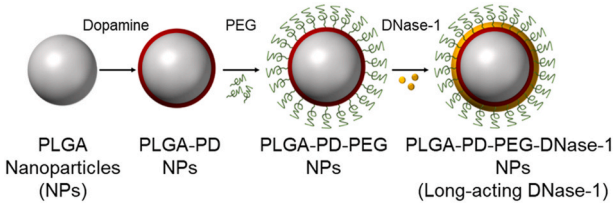

Scheme 1. Preparation of long-acting nanoparticulate DNase-1. Schematic illustration of the preparation of long-acting DNase-1. DNase-1 was immobilized by coating polydopamine on the surface of PLGA NPs.

2. Materials and methods

2.1. Materials

Poly (lactic-co-glycolic acid) (PLGA; lactic acid:glycolic acid = 1:1, viscosity 0.55–0.75 DL/g, Part#: B6013-2P was purchased from Durect Corporation (AL, USA). Poly(vinyl alcohol) (PVA), Tris buffer (pH 8.5) and polydopamine (PD) were obtained from Sigma-Aldrich (PA, USA). Poly (ethylene glycol) (PEG, 4 arm-amine termini, HCL salt) was provided by JenKem, (TX, USA). Dichloromethane (DCM) and DNase-1 were purchased from Daejung (Seoul, South Korea) and Roche (Basel, Switzerland), respectively.

2.2. Preparation of long-acting nanoparticulate DNase-1

Long-acting DNase-1 was prepared as previously described [15,16]. Primary nanoparticles were prepared with the FDA-approved polymer, PLGA, via a conventional single emulsification method (Scheme 1). To prepare bare nanoparticles (PLGA NP), 400 mg PLGA was dissolved in 5 mL DCM and then poured into a 20 mL solution of 1% PVA. The resulting polymer solution was sonicated for 10 min at 40% amplitude with 1 s on and 1 s off using a Q700 sonicator (Qsonica, LLC, Newtown, CT, USA). The prepared emulsions were poured into 5 mL DI water and residual DCM was allowed to evaporate overnight at room temperature with magnetic stirring. The PLGA NPs (400 mg) were resuspended in 20 mL 10 mM, pH 8.5 Tris buffer and coated with a bio-adhesive made of polydopamine (PD, 100 mg dopamine in 1 mL water) with vigorous stirring at 4 °C for 3 h. The bio-adhesive nanoparticles (PLGA-PD NPs) were collected by centrifugation at 17,000 rpm for 20 min, resuspended in 5 mL Tris buffer (10 mM, pH 8.5) containing 50 mg DNase-1 and 50 mg poly(ethylene glycol), and stirred at 4 °C for 3 h. The resulting DNase-1-coated NPs were then collected and washed with DI water to prepare PLGA-PD-PEG-DNase-1 NPs (referred to as long-acting DNase-1).

2.3. Characterization of long-acting nanoparticulate DNase-1

The long-acting DNase-1 was diluted in Milli-Q water and a drop of the solution was placed on a copper grid followed by drying in a vacuum chamber. Upon drying, the grid was carefully placed on a sample holder for analysis using a JEM-7500F (Akishima, Japan) scanning electron microscope (SEM). The size and zeta potential of the particles were measured using a Malvern Zetasizer Nano ZS system (Malvern Instruments, Southborough, MA, USA). The DNAse-1 activity was confirmed using a DNA degradation assay. For this analysis, a 1 kb double-stranded DNA (dsDNA) ladder with sizes ranging 1 kb (New England Biolabs, MA, USA) was used as a substrate for cleavage by the DNase-1endodeoxyribonuclease. Enzymatic activity assays were performed with either free DNase-1 or the long-acting DNase-1 in a final volume of 20 μL of buffer (100 mM sodium acetate, 6.25 mM magnesium sulfate, pH 5.0) containing 2 μg of dsDNA. The reaction was incubated at 37 °C for 10 min followed by the addition of 1 unit of control enzyme, free DNase-1, various concentrations of long-acting DNase-1 (0.1–10

μL), or 10 μL uncoated control NPs (PD-PEG NPs without immobilized DNAse-1 on its surface). After incubation, samples were electrophoresed on a 1% agarose gel and stained with ethidium-bromide (EtBr, 0.5 μg/mL) for 35 min. DNA bands were visualized using a Bio-Rad Chemi Doc XRS + (Hercules, Canada) equipped with standard excitation and emission filters to image the labeled DNA bands. The experiments were repeated at least three times.

2.4. Plasma sample

Whole blood was collected from patients admitted at Yeungnam University Medical Center after they were diagnosed with the SARS-CoV-2 infection at a public health center in Daegu, Republic of Korea. Patients with COVID-19 sepsis were defined using criteria provided by the Sepsis Consensus Conference Committee [17]. Eligible patients met the following criteria: age, over 18 years; and an acute onset medical condition with as at least one of the following criteria: fever (tympanic temperature $\geq$ 38 °C at the nurse triage), suspected systemic infection, two or more systemic inflammatory response syndrome SIRS criteria, hypotension (systolic blood pressure $<$ 90 mmHg), and/or shock. Healthy volunteers were used as controls. Clinical data were collected for all the patients. Plasma samples were prepared by centrifugation at 2000×*g* for 5 min within 12 h after whole blood collection. The human study protocol was approved by the Institutional Review Board of Yeungnam University Hospital at Daegu in Korea (YUH 2020-03-057 and 2020-05-031-001).

2.5. Neutrophil counts of patients with COVID-19

Complete blood counts were obtained from the patients' venous blood samples. The laboratory findings were analyzed within 24 h after admission. Neutrophil count was performed using a Sysmex XE-2100 Automated Hematology System.

2.6. NET enzyme-linked immunosorbent assay (ELISA)

Freshly isolated neutrophils (1×10^5 cells) were stimulated to generate NETs by incubating with 25 nM phorbol-myristate acetate (PMA, Sigma-Aldrich, MO, USA) or control media (RPMI 1640 supplemented with glutamine, penicillin, and streptomycin) and evaluated using a fluorometric technique as previously described [18]. NET production was measured as arbitrary fluorescent units (AFUs).

2.7. MPO ELISA

To quantify the release of granule matrix proteins upon degranulation in peripheral blood mononuclear cells (PBMCs)of SARS-CoV-2-infected patients and mice, plasma were analyzed using a human MPO ELISA kit (BMS2038INST, Invitrogen) and mouse myeloperoxidase ELISA kit (MBS700747, MyBioSource), respectively.

2.8. ELISA and Western blot analysis of Cit-histone H3

Cit-histone H3 concentrations in cell culture media or septic patient sera were determined using a human citrullinated histone H3 ELISA Kit (MBS7254090, MyBioSource). Albumin-removed plasma protein (approximately 20 μg per lane) was separated by sodium dodecyl sulfate-polyacrylamide gel electrophoresis (SDS-PAGE) on 8% polyacrylamide gels and transferred onto nitrocellulose membranes (Bio-Rad Laboratories, Hercules, CA). The membranes were blocked with 0.05% PBS-Tween (PBST) containing 5% bovine serum albumin (BSA) and then incubated with the primary antibody at 4 °C overnight. Bound anti-histone H3 (citrulline R2 + R8 + R17) antibody was detected by incubation with horseradish peroxidase (HRP)-coupled secondary antibody (1:2000 in PBST with 5% BSA) at room temperature for 2 h. Chemiluminescence detection was performed by using Western Lighting Chemiluminescence Reagent Plus (PerkinElmer LAS, Inc., Boston, MA).

2.9. Quantification of plasma cfDNA

For isolation of cfDNA from the plasma of SARS-CoV-2-infected patients or mouse plasma, a Qiagen QIAamp DNA Mini Blood Mini Kit was used according to the manufacturer's instructions (Qiagen, Valencia, CA, USA) after centrifugation of the plasma at 16,800×*g* for 10 min. Purified cfDNA was quantified using a NanoDrop spectrophotometry.

2.10. ELISA for DNase-1 activity

Serum samples were diluted 1:50 with digestion buffer spiked with 1 μg/ml of double stranded DNA. Samples were stained with PicoGreen (Invitrogen) according to the manufacturer's instruction and incubated at 37 °C for 5 h. The reduction in PicoGreen staining (fluorescence emission, Em) was then measured using a fluorometer.

2.11. Neutrophil isolation

PBMCs were isolated on a Percoll (pH 8.5–9.5; Sigma-Aldrich, UK) density gradient as previously described [19]. The PBMCs (95% purity and 97% viable according to trypan blue exclusion) were resuspended in RPMI 1640 media (Sigma-Aldrich). Neutrophils were isolated using discontinuous density gradient centrifugation on 1-step Polymorphs (Axis-Shield, Oslo, Norway). To increase purity, the neutrophil population was further purified using CD45 antibody-conjugated magnetic beads and magnetic-activated cell sorting (MACS). Viability of the neutrophils was generally >95% as assessed by trypan blue dye exclusion. To verify the effect of long-acting DNase-1 on inhibition of cytokine production, neutrophils were isolated from SARS-CoV-2-infected patients and treated with long-acting DNase-1. Long-acting DNase-1 was also administrated septic CLP mice. Supernatants were used for cytokine analyses using ELISA and the cell lysates were used for analysis of NF-kB activity.

2.12. NF-kB activity

Preparation of nuclear extracts and TransAM assays were performed as previously described [20]. The activity of individual NF-κB subunits was determined using an ELISA-based NF-κB Family Transcription Factor Assay Kit (43296; Active Motif, Carlsbad, CA, USA). Briefly, nuclear extracts (2 μg) were incubated in a 96-well plate, which was coated with NF-κB consensus oligonucleotides. The captured complexes were incubated with specific NF-κB primary Abs and subsequently detected using HRP-conjugated secondary Abs included with the kit. Finally, the optical density (OD) at 450 nm was measured using a Tecan Spark microplate reader (Tecan, Austria GmbH, Austria).

2.13. Cytokine ELISAs

Serum levels of inflammatory cytokines IL-1β, IL-6, IFN-γ and TNF-α and LDH were determined in SARS-CoV-2-infected patients and discharged patients using human ELISA kits (Quantikine ELISA, R&D Systems, Minneapolis, MN, USA) according to the manufacturer's instructions. The results were expressed as pg/mL.

2.14. Animals and husbandry

C57BL/6 male mice (six to seven week-old, weighing 18–20 g) were obtained from Orient Bio (Seongnam, Korea) and used after a 12-day acclimatization period. Five animals per cage were housed under controlled temperature at 20–25 °C and humidity of 40–45% with a 12:12 h light/dark cycle. Mice were fed a normal rodent pellet diet and supplied with water *ad libitum*. All animals were treated according to the Guidelines for the Care and Use of Laboratory Animals issued by the

SKKU (No. SKKUIACUC2020-04-34-2).

2.15. Cecal ligation and puncture

The CLP-induced septic mouse model was prepared as previously described [21]. Briefly, a 2-cm midline incision was made to expose the cecum and adjoining intestine. The cecum was then tightly ligated using a 3.0-silk suture 5.0 mm from the cecal tip, punctured with a 22-gauge needle, and then gently squeezed to extrude feces from the perforation site. The cecum was then returned to the peritoneal cavity and the laparotomy site sutured using 4.0-silk. For sham operations, the cecum of animals was surgically exposed but not ligated or punctured and then returned to the abdominal cavity.

2.16. Cell analysis by flow cytometry

To analyze the neutrophils and macrophages that migrated into the peritoneal cavity, CD45-positive PBMCs were isolated by MACS. In the sham group, the number of infiltrated neutrophils and macrophages were minimal, so PBMCs from 5 mice per group were pooled. CD45-positive PBMCs stained neutrophil surface markers FITC conjugated anti-Ly6G and macrophage surface markers APC conjugated anti-F4/80 antibodies. Stained cells were resuspended in 1 mL PBS and the fluorescence was quantified using a FACS flow cytometer (BD Bioscience, VA, USA).

2.17. Hematoxylin & eosin (H&E) staining and histopathological examination

Male C57BL/6 mice underwent CLP and were then intravenously administered free DNase-1 or long-acting DNase-1 (100 units) at 12 h or 24 h after CLP (n = 5). Mice were euthanized 72 h after CLP treatment. To analyze the phenotypic changes in the lungs of the mice, lung specimens were removed from each mouse. H&E staining was performed using a standard protocol.

2.18. Clinical chemistry and cytokine levels in the plasma of septic mice

Fresh serum was used for evaluation of AST, ALT, BUN, creatinine, and LDH levels using biochemical kits (MyBioSource). Values were measured using an ELISA plate reader (Tecan, Austria GmbH, Austria).

2.19. Statistical analysis

All experiments were independently performed at least three times. Statistically significant differences were determined using the unpaired *t*-test. Graphpad Prism software was used for statistical analyses. Data are reported as mean ± SEM with significance set at $P < 0.05$. *P*-values and detailed information for each experiment are provided in the figure legends.

3. Results

3.1. Increased neutrophil counts in COVID-19 patients with sepsis

Patient information and blood samples were collected from individuals infected with SARS-CoV-2 and the blood was analyzed. It has been reported that patients with severe symptoms, especially for those who have progressed to sepsis, undergo lymphopenia and thus have reduced numbers of lymphocytes [22,23]. In addition, increases in

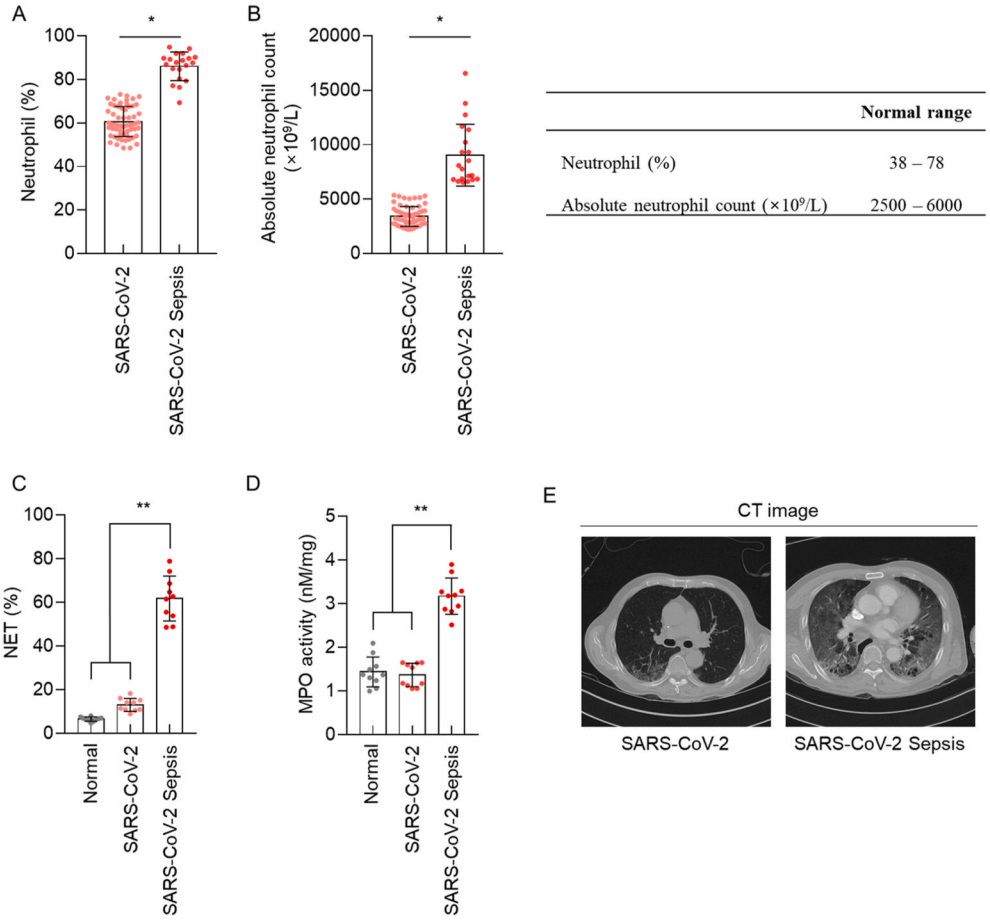

	Normal range
Neutrophil (%)	38 – 78
Absolute neutrophil count (×10⁹/L)	2500 – 6000

Fig. 1. Increased levels of activated neutrophils in SARS-CoV-2-infected patients with sepsis. Comparison of **(A)** neutrophils and **(B)** absolute neutrophil count (ANC) between in SARS-CoV-2-infected patients without sepsis (SARS-CoV-2) and SARS-CoV-2-infected patients with sepsis (SARS-CoV-2 Sepsis). **(C)** NETs (NE-DNA ELISA) and **(D)** MPO activity was quantified in normal control individuals, SARS-CoV-2-infected patients without sepsis, and SARS-CoV-2-infected patients with sepsis. **(E)** CT scans of SARS-CoV-2 and SARS-CoV-2 Sepsis patients. Statistical analysis was performed using a two-tailed unpaired *t*-test. Data are presented as mean ± SEM. *P < 0.05, **P < 0.01.

absolute neutrophil numbers and neutrophil-to-lymphocyte ratios are also usually associated with the severity of diseases [24]. Therefore, we evaluated the neutrophils in SARS-CoV-2-infected patients and observed elevated neutrophil numbers (Fig. 1A). Absolute neutrophil counts were also seen in COVID-19 patients with sepsis (Fig. 1B). Noticeably, the level of activated NET formation (Fig. 1C) and expression of MPO were significantly increased in these patients (Fig. 1D). It has been reported that excessive amounts of NETosis lead to a hyperinflammatory response [25], which subsequently attributes to organ damage and multiple organ failure [26]. In most cases, elderly patients and those individuals with underlying conditions progress toward sepsis [27,28]. Computed tomography (CT) imaging revealed that patients with abnormally high numbers of neutrophils had severe lung tissue damage, indicating an increase in the severity of septic symptoms (Fig. 1E). The diagnosis of pneumonia in COVID-19 patients with sepsis was verified based on lactate dehydrogenase (LDH) levels. LDH levels in the COVID-19 sepsis group were significantly increased compared with those in COVID-19 patients without sepsis (Fig. S1).

3.2. Elevated neutrophil activity in COVID-19 patients with sepsis

Levels of cfDNA were measured in 80 blood samples from COVID-19 patients, including 20 patients with sepsis. Levels of cfDNA were also measured in 20 healthy control volunteers (normal group). The median serum cfDNA level in the normal group was 0.41 (0.25–0.6) μg/mL. In comparison, the level of cfDNA was slightly increased to 0.85 (0.46–1.42 μg/mL) in the 60 SARS-CoV-2-infected patients and drastically increased to 2.83 (2.14–3.39) μg/mL in the 20 COVID-19 patients with sepsis (Fig. 2A). Differences were also observed for DNase-1 levels among the groups. For the normal group, the median DNase-1 was 2.11 (1.59–2.77) μg/mL compared to 3.11 (2.08–6.78) μg/mL for the COVID-19 patients without sepsis and 0.97 (0.52–1.44) μg/mL for the COVID-19 patients with sepsis (Fig. 2B). Analysis of citrullinated histone H3 (Cit-histone H3) levels in the blood samples revealed even more obvious differences. In the normal group, the Cit-histone H3 median level was 0.046 (0.025–0.067) μg/mL compared to 0.304 (0.033–0.971) μg/mL for the COVID-19 patients without sepsis and 17.735 (12.307–22.525) μg/mL for the COVID-19 patients with sepsis (Fig. 2C). We evaluated the expression levels of histone H3 and Cit-histone H3 in the plasma of patients with COVID-19 using Western blot analysis (Fig. 2D). As shown in Fig. 2C and D, Cit-histone H3 levels were increased in the plasma samples of COVID-19 patients with sepsis compared to those without sepsis and healthy volunteers.

The levels of cfDNA, DNase-1, and Cit-histone H3 were re-analyzed in the 80 patients with COVID-19 according to patient end outcome (n = 69 survived and n = 11 deceased). The differences in the levels of cfDNA, DNase-1, and Cit-histone H3 were much more pronounced in the deceased group of patients. Unexpectedly high levels of cfDNA (Fig. 2E) and significantly reduced levels of DNase-1 (Fig. 2F) were observed, as well as increased levels of Cit-histone H3 (Fig. 2G) were observed, especially in the deceased patient group. Treatment is often ineffective for COVID-19 patients with severe sepsis symptoms, even when conventional antiviral drugs against other virus are administered [24].

3.3. Exogeneous DNase-1 reduced NETosis in the plasma of COVID-19 patients with sepsis

Having confirmed the abnormal levels of factors related to NETosis and reduced amounts of endogenous DNase-1 in COVID-19 patients, we then sought to leverage the use of exogenous DNase-1 to suppress the NETosis of neutrophils in effort to compensate for the loss of DNase-1 in patients with COVID-19. Due to the extremely short half-life of DNase-1 in blood [29], we prepared DNase-1-coated nanoparticles as previously described [15,16] to serve as long-acting DNase-1 (Scheme 1 and Fig. 3) since immobilization of DNase-1 on the surface of nanoparticles can enhance the stability of DNase-1 in the blood and thereby improving activity of the DNase-1. Mussel-inspired polydopamine chemistry was utilized to effectively immobilize DNase-1 on the nanoparticle surface [30,31]. SEM analysis showed that PLGA-NPs have a spherical shape with a size of about 170 nm (Fig. 3A). When the PLGA NP surface was

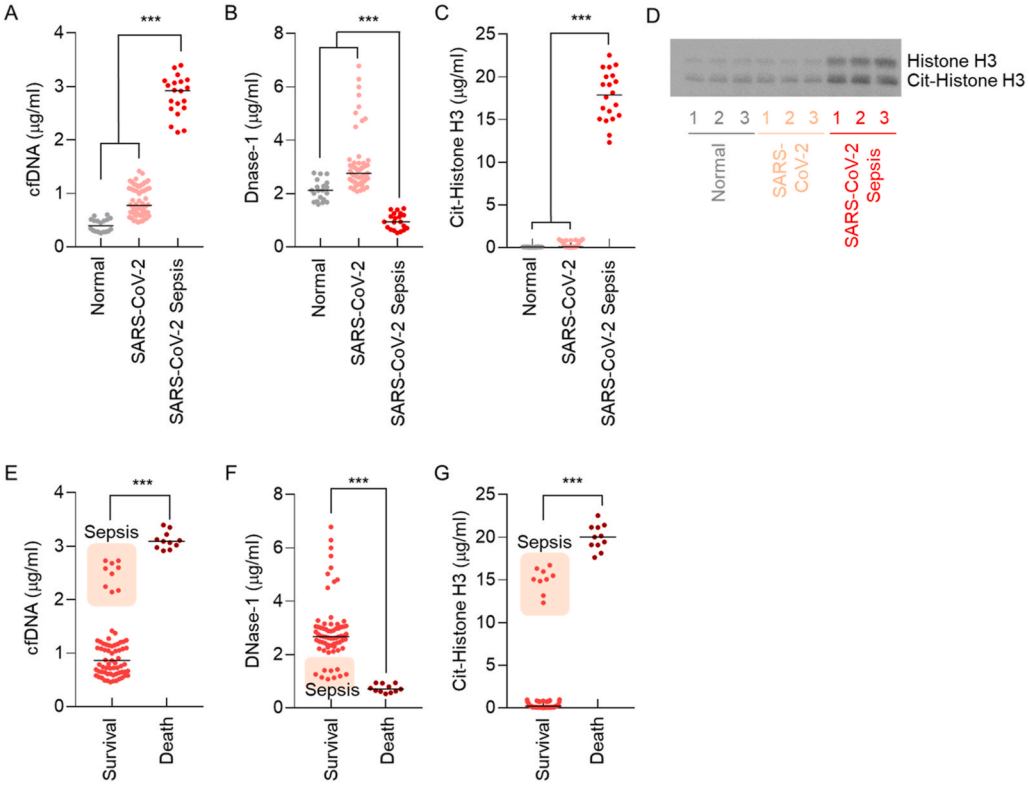

Fig. 2. Changes in cfDNA, DNase-1, and histone H3 level in relation with the severity of the SARS-CoV-2 and survival/death. Plasma samples were secured from 20 healthy volunteers, 60 SARS-CoV-2 patients, and 20 patients who progressed to sepsis (SARS-CoV-2 Sepsis). (**A**) Circulating cfDNA was detected by spectrophotometry (NanoDrop) and (**B**) DNase-1 and (**C**) Histone H3 levels were measured by ELISA. (**D**) Citrullinated histone H3 (Cit-histone H3) was analyzed by Western blot. (**E–F**) Concentration of cfDNA, DNase-1, and histone H3 in SARS-CoV-2 patients. Patients were grouped according to survival or death (**E–G**). Statistics were calculated using a two-tailed unpaired *t*-test. Samples in the colored area (patients with sepsis) were excluded in the survival group for statistical analysis (**E–G**).***$P < 0.001$.

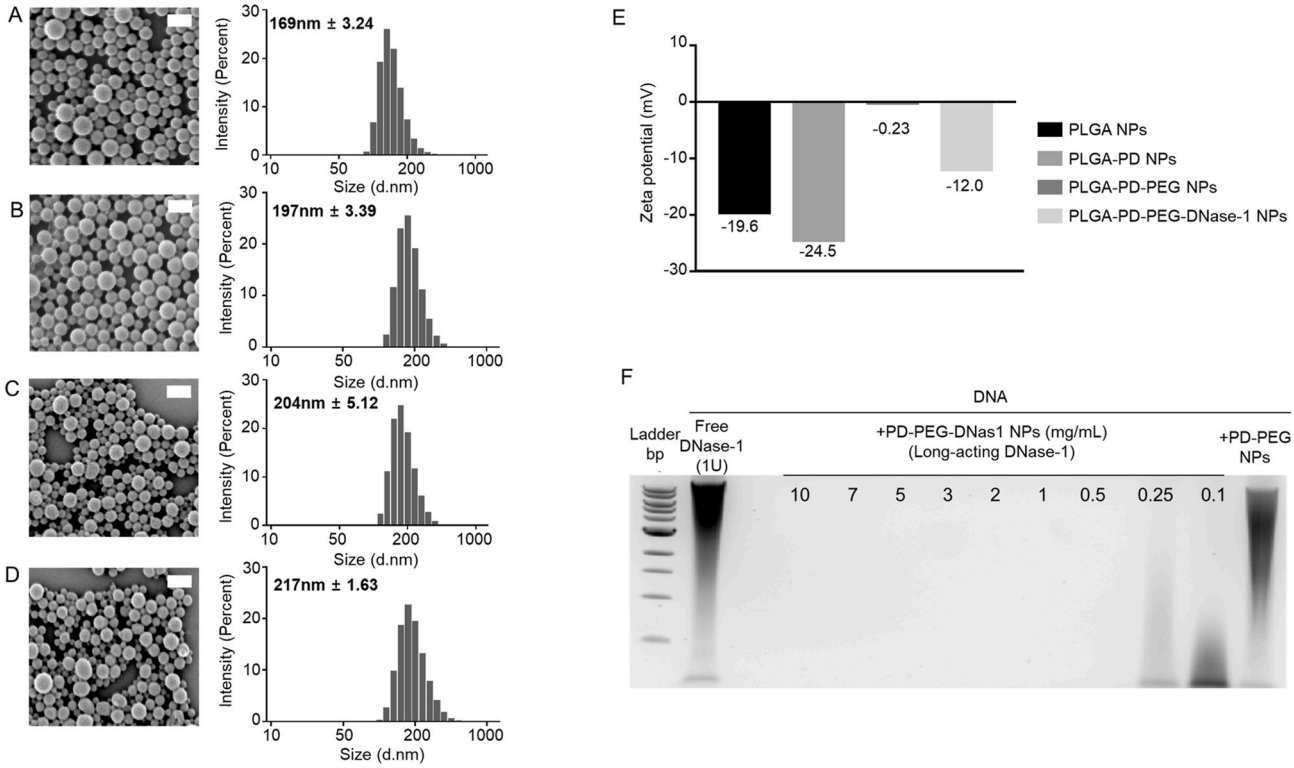

Fig. 3. Physicochemical characterization of long-acting nanoparticulate DNase-1. (A–D) Representative scanning electron micrographs and size distribution of **(A)** PLGA-NPs, **(B)** PLGA-PD-NPs, **(C)** PLGA-PD-PEG NPs, and **(D)** PLGA-PD-PEG-DNase-1 NPs (long-acting DNase-1). Scale bar: 500 nm. The long-acting DNase-1 possessed a smooth spherical shape with an average size of approximately 200 nm. **(E)** Surface charges of PLGA-NPs, PLGA-PD-NPs, PLGA-PD-PEG NPs, and PLGA-PD-PEG-DNase-1 NPs (long-acting DNase-1). The long-acting DNase-1 had a negative charge of −12 mV. **(F)** DNA digestion capability of long-acting DNase-1. Note. Poly (lactic-co-glycolic acid); PLGA, Polydopamine; PD, polyethylene glycol; PEG.

modified with polydopamine and coated with PEG and DNase-1, it was observed that the particle size gradually increased to approximately 220 nm (Fig. 3B–D). The shape of the particles was spherical even after DNase-1 was coated. The surface charge of the nanoparticles was −19.6 mV for PLGA NPs, −24.5 mV for PLGA-PD NPs, −0.2 mV for PLGA-PD-PEG NPs, and −12.0 mV for PLGA-PD-PEG-DNase-1 NPs, respectively (Fig. 3E). DNA digestion was tested to confirm the activity of DNase-1 immobilized on the nanoparticle surface (Fig. 3F). The long-acting DNase-1 effectively degraded DNA at concentrations >0.25 mg/mL. In vitro release test was performed to evaluate the stability of DNase-1 bound on nanoparticles. As shown in Fig. S2, DNase-1 released less than 20% from long-acting DNase-1 for 72 h. Additionally, when the activity of long-acting DNase-1 over time was tested *in vitro*, long-acting DNase-1 stably degrades DNA for up to 36 h (Fig. S3).

To demonstrate the effects of DNase-1 on DNA degradation, we treated the plasma of COVID-19 patients with sepsis with the free DNase-1 and long-acting DNase-1. The results showed that both forms of DNase-1 significantly reduced cfDNA levels (Fig. 4A) and that exposure of DNase-1 to the plasma of COVID-19 patients with sepsis increased the activity of DNase-1 (Fig. 4B). We also observed markedly reduced NET levels, MPO activity, and NE levels in neutrophils of COVID-19 patients with sepsis upon treatment of the DNase-1 formulations (Fig. 4C–E). ARDS and sepsis are common immunopathological phenomena and the leading causes of death for patients infected with SARS-Cov-2 [32,33]. One of the primary mechanisms for ARDS and sepsis in SARS-CoV-2 infection is the cytokine storm [1], which is a deadly uncontrollable systemic inflammatory response resulting from the release of large amounts of pro-inflammatory cytokines and chemokines by immune effector cells [34,35]. Therefore, the effects of DNase-1 on the activation of NF-κB and secretion of cytokines from neutrophils were evaluated. The results showed that the activity of NF-κB and secretion of cytokines IL-1β, IL-6, IFN-γ, and TNF-α were reduced slightly by treatment with free DNase-1 and further decreased by treatment with long-acting DNase-1 (Fig. 4F–J).

3.4. Long-acting DNase-1 reduces NETosis in a septic mouse model

Having confirmed anti-septic activity and reduction in NETosis of neutrophils by treatment with DNase-1 formulations, we extended the effects DNase-1 *in vivo* and aimed to evaluate the utility of such treatments in a therapeutic setting. Based on the hypothesis that reduced neutrophil activation would lead to enhanced survival and be a valid target for preventing or curing sepsis, we tested exogenous administration of the DNase-1 formulations in a cecal ligation and perforation (CLP)-treated septic mouse model (Fig. 5A). The CLP model is an *in vivo* model in which NETosis, CRS, and multiple organ failure (MOF) syndrome can be induced. Because similar phenotypes are also observed in severe cases of SARS-CoV-2-infected patients, the CLP model can be used to represent the SARS-CoV-2-induced sepsis symptoms of patients with COVID-19. With the current limitations and no alternatives being available, the CLP model was considered to be an applicable *in vivo* model for the current setting. To confirm the anti-septic effects of DNase-1, CLP-treated mice were intravenously injected with phosphate-buffered saline (PBS; control group), free DNase-1 (100 units), or long-acting DNase-1 (100 units) at 12 h and 24 h post CLP-treatment. All of the CLP-treated mice died within 78 h of the CLP procedure when no DNase-1 treatment was given, demonstrating the high mortality seen for the CLP-treated sepsis model. Even with the administrations of free DNase-1, the septic mice died quickly with none of the CLP-mice (0%) surviving at 96 h after CLP induction. This lack of an *in vivo* effect of free DNase-1 may have been due to the short half-life of DNase-1 [29]. Intriguingly, the long-acting DNase-1 conferred a 50% survival rate for the CLP-treated septic mice at 96 h. Ultimately, these mice fully recovered.

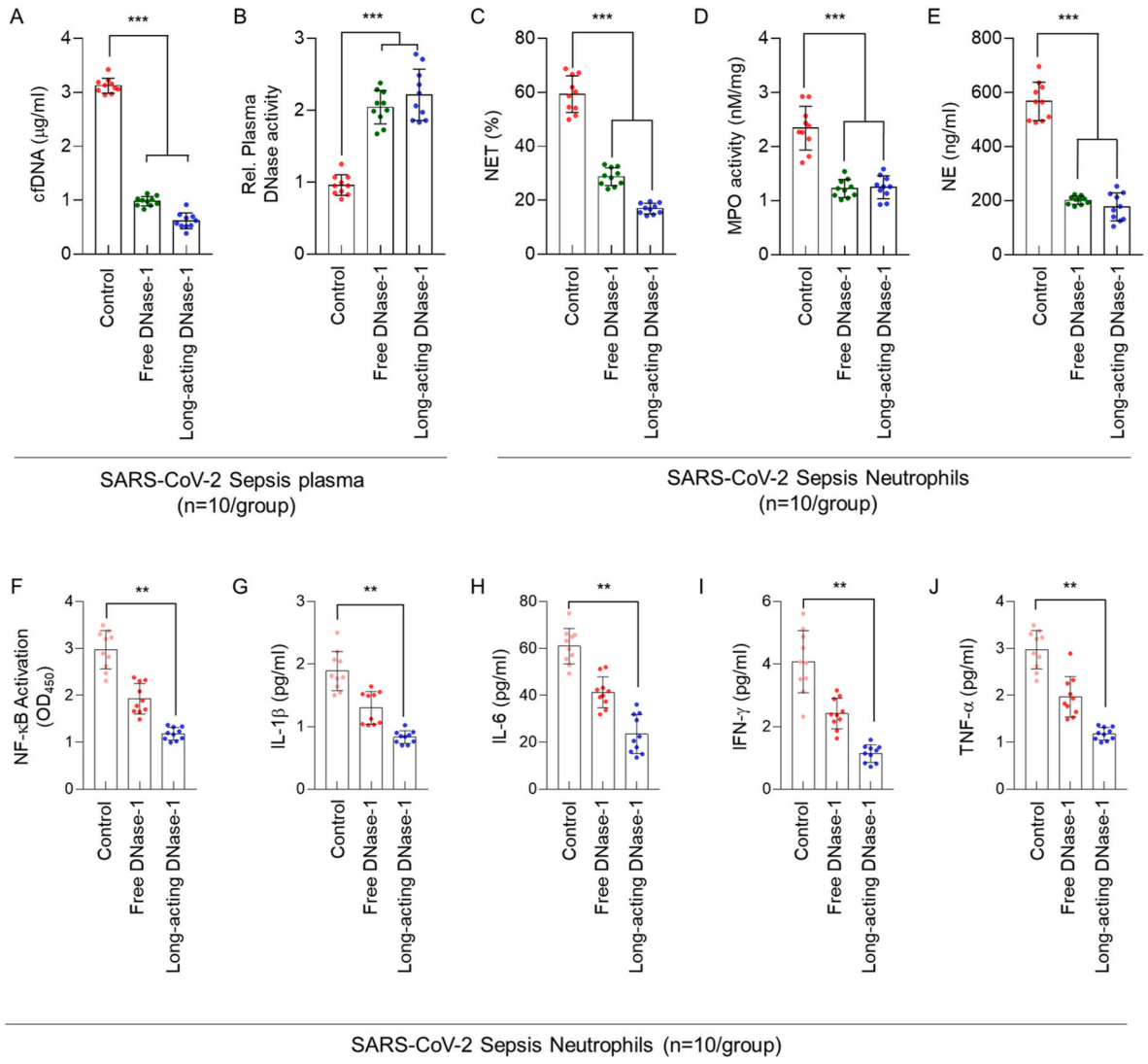

Fig. 4. NETosis index and cytokine production in free DNase-1- or long-acting DNase-1-treated SARS-CoV-2 Sepsis patients' plasma and PBMCs. (A–B) SARS-CoV-2 Sepsis patient plasma was incubated with free DNase-1 (100 units) or long-acting DNase-1 (100 units) for 1 h (each group n = 10). **(A)** cfDNA was isolated from the plasma, and concentration of the cfDNA was measured. **(B)** DNase-1 activity was quantified and compared between PBS, free DNase-1, or long-acting DNase-1. **(C–E)** Purified PBMCs from SARS-CoV-2 Sepsis patient whole blood cultured with free DNase-1 or long-acting DNase-1 for 6 h. NET was characterized by measuring the concentration of myeloperoxidase (MPO) and neutrophil elastase (NE). **(C)** NET ratio of SARS-CoV-2 Sepsis patient PBMCs was suppressed after free DNase-1 or long-acting DNase-1 treatment. **(D)** Free DNase-1 or long-acting DNase-1 reduced the MPO activity in SARS-CoV-2 Sepsis patient PBMCs. **(E)** Concentration of NE in PBMC cultured media was decreased by free DNase-1 or long-acting DNase-1. **(F)** Binding activity of NF-κB p65 in PBMC cultured with PBS, free DNase-1 (100 units, 6 h), or long-acting DNase-1 (100 units, 6 h) was measured using the Trans AM NF-κB p65 assay kit. **(G–J)** Series of comparison of plasma cytokine levels in PBS-, free DNase-1 (100 units, 6 h)-, or long-acting DNase-1 (100 units, 6 h)-treated PBMC of SAR-CoV-2 patients. The experiment was performed with replicates at least three times. Statistical analysis was performed using a two-tailed unpaired *t*-test. Data are presented as mean ± SEM. $^{**}P < 0.01$, $^{***}P < 0.001$.

Recently, remdesivir has been approved by the FDA and growing evidences support the use of corticosteroid and dexamethasone for the treatment of COVID-19 patients. To evaluate the combinatorial therapeutic effects of the dexamethasone and nanoparticulate DNase-1, CLP-treated mice were intravenously injected with phosphate-buffered saline, dexamethasone, long-acting DNase-1, or dexamethasone + long-acting DNase-1 at 12 h and 24 h post CLP-treatment (Fig. S4). In the experiment, 2.5 mg/kg of dexamethasone was used [36]. When no dexamethasone or DNase-1 was given, all of the CLP-treated mice died within 78 h of the CLP procedure as demonstrated in Fig. 5A. However, with the administrations of dexamethasone, 40% of septic mice survived at 132 h after CLP induction. Similarly, with the administrations of long-acting DNase-1, 50% of septic mice survived at 132 h after CLP induction. Intriguingly, the dexamethasone + long-acting DNase-1 conferred a 60% survival rate for the CLP-treated septic mice at 132 h.

We then evaluated the number of neutrophils present in the peritoneal cavity of the mice. It was evident that the long-acting DNase-1 induced a drastic reduction (almost half) in the number of peritoneal neutrophils compared to the control group (PBS treatment) and free DNase-1 group (Fig. 5B). Having inducing an anti-septic effect using the long-acting DNase-1, we then aimed to determine whether this treatment could specifically reduce the infiltration of $Ly6G^+$ neutrophils to peritoneal cavity. Increased numbers of $Ly6G^+$ neutrophils were observed in the control group, but free DNase-1 and long-acting DNase-1 treatment led to a substantial decrease in the number of infiltrating $Ly6G^+$ neutrophils (Fig. 5C). Previously, it was reported that Ly6G-expressing ($Ly6G^+$) neutrophils increase secretion of various cytokines and chemokines. They capture and destroy invading microorganisms, through phagocytosis and intracellular degradation, thereby releasing granules and forming neutrophil extracellular traps (NETs) after

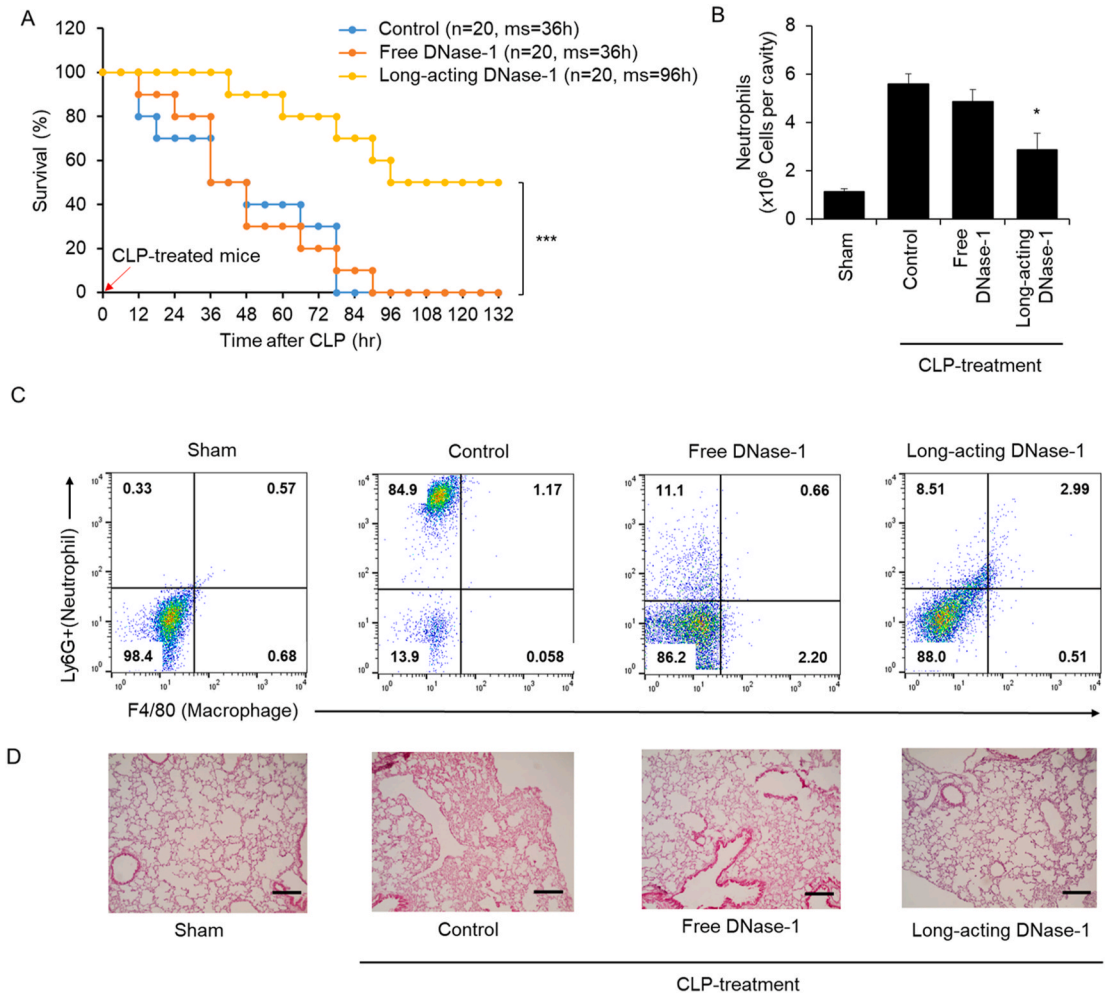

Fig. 5. Anti-septic effects of long-acting DNase-1. Male C57BL/6 mice (n = 60/group pooled from 3 independent experiments) were administered PBS, free DNase-1 (100 units), or long-acting DNase-1 (100 units) 12 h and 24 h after CLP. **(A)** Kaplan-Meier curves of CLP mice administered with PBS, DNase-1 (100 units), or long-acting DNase-1 (100 units). **(B)** CLP-mediated migration of neutrophils into the peritoneal cavity of mice was analyzed after treating mice with PBS, free DNase-1 (100 units), or long-acting DNase-1 (100 units). **(C)** Flow cytometry analysis. Free DNase-1 and long-acting DNase-1 were administered 12 h after CLP surgery and peritoneal fluid collected 2 h later. PBMCs in the peritoneal fluid were separated by MACS using a CD45 antibody. Purified PBMCs stained with neutrophil surface markers; FITC-conjugated anti-Ly6G and macrophage surface markers APC-conjugated anti-F4/80 antibodies. **(D)** Histologic changes in the lung 3 d after CLP treatment. Scale bar, 20 μm. The experiment was performed at least three times with replicates. Statistical analysis was performed using a two-tailed unpaired *t*-test. The log-rank (Mantel-Cox) test was used for statistical analysis of survival. Data are presented as mean ± SEM. *P < 0.05, ***P < 0.001.

detecting pathogens [37]. It is considered that abundant lung-infiltrating neutrophils in acute lung injury (ALI) or acute respiratory distress syndrome (ARDS) also participate as mediators of inflammation. We also confirmed that the long-acting DNase-1, which acts on the lungs, substantially reduced the morphological changes caused by CLP, including pulmonary edema, hemorrhage, alveolar collapse, and inflammatory cell infiltration (Fig. 5D). To further support the acting of long acting DNase-1 on the lungs, we evaluated the biodistribution of nanoparticulate DNase-1 (Fig. S5). Mice were intravenously injected with fluorescently-labeled free DNase-1 or long-acting DNase-1 and analyzed at 6 h, 12 h, and 24 h post treatment. Unsurprisingly, the long acting of DNase-1 was predominantly accumulated in the liver and kidney due to the mononuclear phagocytic system (MPS) [38–40]. Interestingly, the long acting of DNase-1 was accumulated in the lung and was cleared after 24 h, suggesting sufficient time for biological activity *in vivo*. As for the free DNase-1, some accumulation in the lung was observed, but it was soon cleared after 12 h.

We also verified the effect of the DNase-1 formulations on the degradation of DNA in the plasma using the CLP septic mouse model. Similar to the plasma of COVID-19 patients with sepsis, the long-acting DNase-1 significantly reduced cfDNA levels and increased the activity of the DNase-1 (Fig. S6A and B). Additionally, significant reductions in NET, MPO activity, NE levels, and neutrophil numbers were observed upon treatment with the long-acting DNase-1 (Fig. S6C–F).

Next, we attempted to elucidate the effect of the long-acting DNase-1 on the regulation of inflammatory responses during sepsis. Systemic inflammation associated with sepsis often causes multiple organ failure [41] with the kidney and liver being the major organs targeted [42]. CLP treatment significantly increased serum levels of hepatic injury markers aspartate transaminase (AST) and alanine transferase (ALT), renal injury markers creatinine and blood urea nitrogen (BUN), the tissue injury marker lactate dehydrogenase (LDH), and the pneumonia and sepsis marker C-reactive protein (CRP) (Fig. S7). Serum levels of these makers were significantly reduced by treatment with the long-acting DNase-1.

4. Discussion

The complex pathophysiology of sepsis is characterized by multiple organ failure caused by hyper inflammation and CRS. The organ failure is accompanied by an immunosuppressive state, which results in a failure to return to normal homeostasis. These events have hampered the development of therapeutic agents that can effectively treat the complex

process of sepsis. It has been reported that SARS-CoV-2 infection can activate both innate and adaptive immune responses [43]. Similar uncontrollable innate inflammatory responses and impaired adaptive immune responses have been shown to be induced by SARS-CoV-2, which results in increased tissue damage, both locally and systemically [44]. In patients with severe COVID-19, lymphopenia has also been observed with a collective and representative characteristic accompanied by an increased ratio of neutrophils and increase in the absolute neutrophil count [22,23]. However, these attributes have not been observed in patients with mild COVID-19 disease. These phenomena are most often associated with increased disease severity and therefore the prognosis is usually a poor clinical outcome.

In our current findings, elevated levels of NETosis markers were observed, such as cfDNA [45], MPO [46], and NE [25]. These are characteristic features of patients critically ill with COVID-19 [47]. It is particularly challenging to treat patients with high levels of NETosis, which is why it is linked to high morbidity and mortality. Therefore, an innovative NETosis-targeting agent that is able to reduce the level of NETosis in the blood and prevent further progression toward sepsis is urgently needed. The observation of similar pathophysiology in sepsis and phenomena seen in patients with COVID-19 led us to the hypothesis that NETosis markers may be useful as possible targets for treatment of patients infected with SARS-CoV-2. The fact that the use of corticosteroids as a treatment for SARS-CoV-2 is not recommended highlights the urgent need for an alternative mean of treating SARS-CoV-2-infected individuals that can effectively suppress hyperinflammation-mediated organ damage that is observed in critically ill patients [48].

Here, we report the effects of exogenous long-acting nanoparticulate DNase-1 on resolving inflammatory responses and reducing organ damage in a CLP-induced septic mouse model. Immobilization of the enzyme on the nanoparticle surface greatly improves the stability of the enzyme [49]. In previous study, DNase-1 coated nanoparticles increased plasma enzyme concentrations compared to native DNase-1 [16]. This means that the short half-life of DNase-1 can be improved by the immobilization on the nanoparticles. Thus, we adopted the DNase-1 coated nanoparticles as long-acting DNase-1 in this study. Indeed, long-acting DNase-1 showed long-term enzymatic activity *in vitro* (Fig. S3), and when injected into the body, DNase-1 coated nanoparticles were expelled through kidney and liver more slowly than native DNase-1 (Fig. S5).

We also performed a comparative study using blood samples from patients with COVID-19 and demonstrated the suppression of neutrophil activity and cytokine levels. Through the administration of long-acting DNase-1 in the septic mouse model, we demonstrated that DNase-1 could effectively reduce sepsis-associated NETosis factors. Our results demonstrated that the long-acting DNase-1 treatment significantly reduced markers cfDNA, NET, MPO, and NE (Fig. S6) in the CLP-induced septic mice. Notably, the long-acting DNase-1 conferred a 50% survival rate for the CLP-treated septic mice at 96 h post procedure (Fig. 5), demonstrating that the mice had fully recovered. This indicated that the treatment, if administered during the early phase of sepsis, may slow progression toward the septic state.

Targeting inflammatory neutrophils using nanoparticles for their apoptosis may be an alternative to treat sepsis. Recently, Zhang, C. Y. et al., reported doxorubicin (DOX)–conjugated protein nanoparticles (NPs) that selectively target inflammatory neutrophils to induce apoptosis of neutrophils [13]. In this study, we used DNase-1, which can inhibit and inactivate NETosis for neutralization of neutrophils. Similar to previous study, we generated long-acting DNase-1 that can suppress the function of neutrophils and verified the efficacy in septic mouse model.

Current antivirals and antimalarials that are being used in clinical trials for the treatment of SARS-CoV-2 have shown therapeutic efficacy in only patients with mild disease and not in critically ill patients with ARDS or sepsis. Our results suggest that DNase-1 could be used as a treatment to inhibit cytokine release and multiple organ dysfunctions in critically ill patients with COVID-19 via suppression of neutrophil activity. Our suggestion is based on results obtained from our current *in vivo* studies using the septic mouse model as a surrogate for SARS-CoV-2 infection. We found that treatment with long-acting DNase-1 significantly decreased NETosis according to levels of markers cfDNA, NET, MPO, and NE (Fig. 4). NF-κB activation and cytokine levels are known to be associated with induced septic inflammation responses. As expected, our results showed that the long-acting DNase-1 inhibited NF-κB activation and cytokine levels. It should be noted that because the CLP-induced mice model was used, the efficacy of long-acting DNase-1 needs to be further validated in an appropriate *in vivo* setting using a virus infection-induced animal model before moving forward to clinical trials on patients with COVID-19.

5. Conclusions

Based on our data from SARS-CoV-2-infected sepsis patients we determined that the NETosis factor, cfDNA, could be a potential therapeutic target for the treatment of virus-induced sepsis. We suggest the therapeutic delivery of a long-acting nanoparticulate DNase-1 formulation for slowing the progression of sepsis in SARS-CoV-2-infected patients by suppressing cfDNA. We confirmed the effectiveness of the long-acting DNase-1 in a septic mouse model, as well as in blood samples collected from actual COVID-19 patients. Long-acting DNase-1 is a promising vehicle and represents a potentially new option for sepsis therapy. No methods targeting the NETosis marker have been previously established with SARS-CoV-2 patient blood samples. Our findings implicate long-acting DNase-1 to possibly be employed as a versatile alternative approach in preventing the further progression of sepsis in patients with COVID-19. Our findings open the possibility of NETosis markers being used as diagnostic targets in SARS-CoV-2-patients with severe COVID-19.

Data availability

All data obtained from this study are included in the article or uploaded as supplementary information. The data that support the findings of this research are available from the corresponding authors upon reasonable request.

CRediT authorship contribution statement

Yun Young Lee: Methodology, Formal analysis, Investigation. **Hee Ho Park:** Resources, Investigation, Writing - review & editing. **Wooram Park:** Investigation, Methodology, Formal analysis, Writing - review & editing. **Hyelim Kim:** Methodology, Formal analysis, Investigation. **Jong Geol Jang:** Resources, Formal analysis. **Kyung Soo Hong:** Resources, Formal analysis. **Jae-Young Lee:** Investigation. **Hee Seung Seo:** Methodology. **Dong Hee Na:** Formal analysis. **Tae-Hyung Kim:** Conceptualization, Methodology. **Young Bin Choy:** Conceptualization, Investigation. **June Hong Ahn:** Resources, Investigation, Formal analysis. **Wonhwa Lee:** Conceptualization, Visualization, Writing - review & editing. **Chun Gwon Park:** Conceptualization, Visualization, Writing - review & editing.

Declaration of competing interest

The authors declare that they have no known competing financial interests or personal relationships that could have appeared to influence the work reported in this paper.

Acknowledgments

This work was supported by the National Research Foundation of Korea (NRF) grant funded by the Korea government (MSIT) (2019R1C1C1006300, 2019R1A4A1028700, 2018R1C1B6001120,

2018M3A7B4071204, 2020R1A4A3078645, and 2020R1A4A4079817). "This work was also supported by the BK21 FOUR Project."

Appendix A. Supplementary data

Supplementary data to this article can be found online at https://doi.org/10.1016/j.biomaterials.2020.120389.

References

[1] P. Mehta, D.F. McAuley, M. Brown, E. Sanchez, R.S. Tattersall, J.J. Manson, COVID-19: consider cytokine storm syndromes and immunosuppression, Lancet 395 (10229) (2020) 1033–1034.

[2] J.L. Vincent, F.S. Taccone, Understanding pathways to death in patients with COVID-19, Lancet Respir Med 8 (5) (2020) 430–432.

[3] Y.X. Du, X.P. Chen, Favipiravir: pharmacokinetics and concerns about clinical trials for 2019-nCoV infection, Clin. Pharmacol. Ther. 108 (2) (2020) 242–247.

[4] H. Li, Y. Zhou, M. Zhang, H. Wang, Q. Zhao, J. Liu, Updated approaches against SARS-CoV-2, Antimicrob. Agents Chemother. 64 (6) (2020) e00483-20.

[5] M. Wang, R. Cao, L. Zhang, X. Yang, J. Liu, M. Xu, Z. Shi, Z. Hu, W. Zhong, G. Xiao, Remdesivir and chloroquine effectively inhibit the recently emerged novel coronavirus (2019-nCoV) in vitro, Cell Res. 30 (3) (2020) 269–271.

[6] Y. Zhou, Y. Hou, J. Shen, Y. Huang, W. Martin, F. Cheng, Network-based drug repurposing for novel coronavirus 2019-nCoV/SARS-CoV-2, Cell Discov. 6 (2020) 14.

[7] J. Phua, L. Weng, L. Ling, M. Egi, C.M. Lim, J.V. Divatia, B.R. Shrestha, Y.M. Arabi, J. Ng, C.D. Gomersall, M. Nishimura, Y. Koh, B. Du, G. Asian Critical Care Clinical Trials, Intensive care management of coronavirus disease 2019 (COVID-19): challenges and recommendations, Lancet Respir Med 8 (5) (2020) 506–517.

[8] S.-S. Jean, P.-I. Lee, P.-R. Hsueh, Treatment options for COVID-19: the reality and challenges, J. Microbiol. Immunol. Infect. 53 (3) (2020) 436–443.

[9] C.D. Russell, J.E. Millar, J.K. Baillie, Clinical evidence does not support corticosteroid treatment for 2019-nCoV lung injury, Lancet 395 (10223) (2020) 473–475.

[10] V. Papayannopoulos, Neutrophil extracellular traps in immunity and disease, Nat. Rev. Immunol. 18 (2) (2018) 134–147.

[11] A. Ma, P. Kubes, Platelets, neutrophils, and neutrophil extracellular traps (NETs) in sepsis, J. Thromb. Haemostasis 6 (3) (2008) 415–420.

[12] E. Lefrancais, B. Mallavia, H. Zhuo, C.S. Calfee, M.R. Looney, Maladaptive role of neutrophil extracellular traps in pathogen-induced lung injury, JCI Insight 3 (3) (2018) 98178.

[13] C.Y. Zhang, X. Dong, J. Gao, W. Lin, Z. Liu, Z. Wang, Nanoparticle-induced neutrophil apoptosis increases survival in sepsis and alleviates neurological damage in stroke, Sci. Adv. 5 (11) (2019), eaax7964.

[14] D.F. Colón, C.W. Wanderley, M. Franchin, C.M. Silva, C.H. Hiroki, F. V. Castanheira, P.B. Donate, A.H. Lopes, L.C. Volpon, S.K. Kavaguti, Neutrophil extracellular traps (NETs) exacerbate severity of infant sepsis, Crit. Care 23 (1) (2019) 113.

[15] J. Albrengues, M.A. Shields, D. Ng, C.G. Park, A. Ambrico, M.E. Poindexter, P. Upadhyay, D.L. Uyeminami, A. Pommier, V. Küttner, Neutrophil extracellular traps produced during inflammation awaken dormant cancer cells in mice, Science 361 (6409) (2018), eaao4227.

[16] J. Park, R.W. Wysocki, Z. Amoozgar, L. Maiorino, M.R. Fein, J. Jorns, A.F. Schott, Y. Kinugasa-Katayama, Y. Lee, N.H. Won, Cancer cells induce metastasis-supporting neutrophil extracellular DNA traps, Sci. Transl. Med. 8 (361) (2016), 361ra138.

[17] M. Singer, C.S. Deutschman, C.W. Seymour, M. Shankar-Hari, D. Annane, M. Bauer, R. Bellomo, G.R. Bernard, J.-D. Chiche, C.M. Coopersmith, The third international consensus definitions for sepsis and septic shock (Sepsis-3), J. Am. Med. Assoc. 315 (8) (2016) 801–810.

[18] J. Hazeldine, P. Harris, I.L. Chapple, M. Grant, H. Greenwood, A. Livesey, E. Sapey, J.M. Lord, Impaired neutrophil extracellular trap formation: a novel defect in the innate immune system of aged individuals, Aging Cell 13 (4) (2014) 690–698.

[19] E. Sapey, H. Greenwood, G. Walton, E. Mann, A. Love, N. Aaronson, R.H. Insall, R. A. Stockley, J.M. Lord, Phosphoinositide 3-kinase inhibition restores neutrophil accuracy in the elderly: toward targeted treatments for immunosenescence, Blood 123 (2) (2014) 239–248.

[20] J. Xu, P. Zhou, W. Wang, A. Sun, F. Guo, RelB, together with RelA, sustains cell survival and confers proteasome inhibitor sensitivity of chronic lymphocytic leukemia cells from bone marrow, J. Mol. Med. 92 (1) (2014) 77–92.

[21] D. Rittirsch, M.S. Huber-Lang, M.A. Flierl, P.A. Ward, Immunodesign of experimental sepsis by cecal ligation and puncture, Nat. Protoc. 4 (1) (2009) 31–36.

[22] T. Wang, Z. Du, F. Zhu, Z. Cao, Y. An, Y. Gao, B. Jiang, Comorbidities and multi-organ injuries in the treatment of COVID-19, Lancet 395 (10228) (2020) e52.

[23] Y. Xu, X. Li, B. Zhu, H. Liang, C. Fang, Y. Gong, Q. Guo, X. Sun, D. Zhao, J. Shen, Characteristics of pediatric SARS-CoV-2 infection and potential evidence for persistent fecal viral shedding, Nat. Med. 26 (4) (2020) 502–505.

[24] B. Zhang, X. Zhou, C. Zhu, F. Feng, Y. Qiu, J. Feng, Q. Jia, Q. Song, B. Zhu, J. Wang, Immune Phenotyping Based on Neutrophil-To-Lymphocyte Ratio and IgG Predicts Disease Severity and Outcome for Patients with COVID-19, medRxiv, 2020.

[25] S.K. Jorch, P. Kubes, An emerging role for neutrophil extracellular traps in noninfectious disease, Nat. Med. 23 (3) (2017) 279–287.

[26] P.G. Czaikoski, J.M.S.C. Mota, D.C. Nascimento, F. Sônego, F.V.e.S. Castanheira, P. H. Melo, G.T. Scortegagna, R.L. Silva, R. Barroso-Sousa, F.O. Souto, Neutrophil extracellular traps induce organ damage during experimental and clinical sepsis, PloS One 11 (2) (2016), e0148142.

[27] G. Onder, G. Rezza, S. Brusaferro, Case-fatality Rate and Characteristics of Patients Dying in Relation to COVID-19 in Italy, JAMA, 2020.

[28] Z. Wu, J.M. McGoogan, Characteristics of and Important Lessons from the Coronavirus Disease 2019 (COVID-19) Outbreak in China: Summary of a Report of 72 314 Cases from the Chinese Center for Disease Control and Prevention, JAMA, 2020.

[29] W. Prince, D. Baker, A. Dodge, A. Ahmed, R. Chestnut, D. Sinicropi, Pharmacodynamics of recombinant human DNase I in serum, Clin. Exp. Immunol. 113 (2) (1998) 289–296.

[30] X. Liu, J. Cao, H. Li, J. Li, Q. Jin, K. Ren, J. Ji, Mussel-inspired polydopamine: a biocompatible and ultrastable coating for nanoparticles in vivo, ACS Nano 7 (10) (2013) 9384–9395.

[31] H. Lee, S.M. Dellatore, W.M. Miller, P.B. Messersmith, Mussel-inspired surface chemistry for multifunctional coatings, Science 318 (5849) (2007) 426–430.

[32] C. Huang, Y. Wang, X. Li, L. Ren, J. Zhao, Y. Hu, L. Zhang, G. Fan, J. Xu, X. Gu, Clinical features of patients infected with 2019 novel coronavirus in Wuhan, China, Lancet 395 (10223) (2020) 497–506.

[33] F. Zhou, T. Yu, R. Du, G. Fan, Y. Liu, Z. Liu, J. Xiang, Y. Wang, B. Song, X. Gu, Clinical course and risk factors for mortality of adult inpatients with COVID-19 in Wuhan, China: a retrospective cohort study, Lancet 395 (10229) (2020) 1054–1062.

[34] R. Channappanavar, S. Perlman, Pathogenic Human Coronavirus Infections: Causes and Consequences of Cytokine Storm and Immunopathology, Semin Immunopathol, Springer, 2017, pp. 529–539.

[35] Q. Liu, Y.-h. Zhou, Z.-q. Yang, The cytokine storm of severe influenza and development of immunomodulatory therapy, Cell. Mol. Immunol. 13 (1) (2016) 3–10.

[36] M.F. Osuchowski, J. Connett, K. Welch, J. Granger, D.G. Remick, Stratification is the key: inflammatory biomarkers accurately direct immunomodulatory therapy in experimental sepsis, Crit. Care Med. 37 (5) (2009) 1567.

[37] M.K. Sercundes, L.S. Ortolan, D. Debone, P.V. Soeiro-Pereira, E. Gomes, E. H. Aitken, A.C. Neto, M. Russo, M.R. D'Imperio Lima, J.M. Alvarez, Targeting neutrophils to prevent malaria-associated acute lung injury/acute respiratory distress syndrome in mice, PLoS Pathog. 12 (12) (2016), e1006054.

[38] W. Poon, Y.-N. Zhang, B. Ouyang, B.R. Kingston, J.L. Wu, S. Wilhelm, W.C. Chan, Elimination pathways of nanoparticles, ACS Nano 13 (5) (2019) 5785–5798.

[39] K.M. Tsoi, S.A. MacParland, X.-Z. Ma, V.N. Spetzler, J. Echeverri, B. Ouyang, S. M. Fadel, E.A. Sykes, N. Goldaracena, J.M. Kaths, Mechanism of hard-nanomaterial clearance by the liver, Nat. Mater. 15 (11) (2016) 1212–1221.

[40] S. Wilhelm, A.J. Tavares, Q. Dai, S. Ohta, J. Audet, H.F. Dvorak, W.C. Chan, Analysis of nanoparticle delivery to tumours, Nat. Rev. Mater. 1 (5) (2016) 1–12.

[41] J.-F. Timsit, E. Azoulay, C. Schwebel, P.E. Charles, M. Cornet, B. Souweine, K. Klouche, S. Jaber, J.-L. Trouillet, F. Bruneel, Empirical micafungin treatment and survival without invasive fungal infection in adults with ICU-acquired sepsis, Candida colonization, and multiple organ failure: the EMPIRICUS randomized clinical trial, J. Am. Med. Assoc. 316 (15) (2016) 1555–1564.

[42] P. Strnad, F. Tacke, A. Koch, C. Trautwein, Liver—guardian, modifier and target of sepsis, Nat. Rev. Gastroenterol. Hepatol. 14 (1) (2017) 55–66.

[43] S.F. Pedersen, Y.-C. Ho, SARS-CoV-2: a storm is raging, J. Clin. Invest. 130 (5) (2020) 2202–2205.

[44] X. Cao, COVID-19: immunopathology and its implications for therapy, Nat. Rev. Immunol. 20 (5) (2020) 269–270.

[45] A. Paunel-Görgülü, M. Wacker, M. El Aita, S. Hassan, G. Schlachtenberger, A. Deppe, Y.-H. Choi, E. Kuhn, T.O. Mehler, T. Wahlers, cfDNA correlates with endothelial damage after cardiac surgery with prolonged cardiopulmonary bypass and amplifies NETosis in an intracellular TLR9-independent manner, Sci. Rep. 7 (1) (2017) 1–13.

[46] D.N. Douda, L. Yip, M.A. Khan, H. Grasemann, N. Palaniyar, Akt is essential to induce NADPH-dependent NETosis and to switch the neutrophil death to apoptosis, Blood 123 (4) (2014) 597–600.

[47] M.N. Bangash, J. Patel, D. Parekh, COVID-19 and the liver: little cause for concern, Lancet Gastroenterol. Hepatol. 5 (6) (2020) 529–530.

[48] W. Alhazzani, M.H. Møller, Y.M. Arabi, M. Loeb, M.N. Gong, E. Fan, S. Oczkowski, M.M. Levy, L. Derde, A. Dzierba, Surviving Sepsis Campaign: guidelines on the management of critically ill adults with Coronavirus Disease 2019 (COVID-19), Crit. Care Med. 46 (5) (2020) 854–887.

[49] M.E. Davis, Z.G. Chen, D.M. Shin, Nanoparticle therapeutics: an emerging treatment modality for cancer, Nat. Rev. Drug Discov. 7 (9) (2008) 771–782.